# Transition to the "island of inversion": Fast-beam $\gamma$-ray spectroscopy of $^{28,30}$Na

B.V. Pritychenko[1,2*], T. Glasmacher[1,2], P.D. Cottle[3] R.W. Ibbotson[1†],
K.W. Kemper[3], K.L. Miller[1,2], L.A. Riley[4], and H. Scheit[1,2‡]

[1] *National Superconducting Cyclotron Laboratory,*
*Michigan State University,*
*East Lansing, Michigan 48824*

[2] *Department of Physics and Astronomy,*
*Michigan State University,*
*East Lansing, Michigan 48824*

[3] *Department of Physics,*
*Florida State University,*
*Tallahassee, Florida 32306*

[4] *Department of Physics and Astronomy,*
*Earlham College,*
*Richmond, Indiana 47374*

(Dated: May 17, 2002)

* Present address: Plumtree Software, Inc., San Francisco, CA 94111
† Present address: Brookhaven National Laboratory, Upton, New York 11973
‡ Present address: Max-Planck-Institut für Kernphysik, Postfach 10 39 80, D-69029 Heidelberg, Germany

## Abstract

The excitation cross sections to the first collective excitations in $^{28,30}$Na have been measured with the technique of intermediate-energy heavy-ion scattering. The trends in the deduced intrinsic electromagnetic quadrupole moments obtained in the present study and in a previous study of $^{31}$Na suggest that the ground state of $^{31}$Na is dominated by intruder configurations, while the lighter sodium isotopes are not. This conclusion is supported by data on binding energies.



PACS numbers: 27.30.+t, 25.70.Bc, 25.70.De

The "island of inversion" phenomenon in neutron-rich exotic nuclei near $N = 20$ is providing a rigorous challenge for our understanding of the evolution of shell structure in isotopes far from stability. This phenomenon, in which several $N = 20$ nuclei ($^{30}$Ne, $^{31}$Na, $^{32}$Mg) have strongly deformed ground state shapes despite having a "magic number" of neutrons (for example, see [1–9]), appears to represent a particularly interesting case of shape coexistence, which occurs throughout the nuclear chart. Shape coexistence at shell closures, which has been observed in nuclei as heavy as the lead isotopes [10], can be described as follows: The "normal" spherical configuration of a nucleus having a closed shell or nearly closed shell lies close in energy to a deformed "intruder" configuration which is formed by promoting a pair of nucleons across the shell closure. Generally, the ground state is dominated by the spherical configuration because energy is required to promote the pair of nucleons across the shell gap. The deformed configurations in $^{30}$Ne, $^{31}$Na, $^{32}$Mg and several $N = 21 - 22$ neighbors result from promotions of neutrons across the $N = 20$ shell closure. The "inversion", in which the deformed configuration becomes the ground state, has been attributed to strong interactions between the promoted neutrons and valence protons, interactions between the promoted neutrons themselves, and shifts in single particle energies [1, 7].

In the present work, we report an experimental study of the transition from "normal" to "inverted" configurations in isotopes of sodium with $N < 20$. We measured low-lying collective excitations of the $N = 17$ and $N = 19$ isotopes $^{28,30}$Na using intermediate energy heavy-ion scattering, which allows the determination of electromagnetic matrix elements. An examination of the present results, a study of $^{31}$Na previously reported [8], and available information on masses demonstrates that the ground states of the $N = 17$ and 19 Na isotopes are *not* "inverted" as in $^{31}$Na, and thus should not be included in the "island of inversion".

The technique of intermediate energy heavy-ion scattering has been used to determine excitation energies and electromagnetic matrix elements in exotic nuclei with masses as high as $A = 60$ (for a review, see [11]). In the region near the island of inversion, this technique has been utilized for studies of the $N = 20 - 21$ isotopes $^{31}$Na [8], $^{32}$Mg [3, 6, 12], $^{33}$Mg [13], and $^{34}$Si [4], the even-even Ne and Mg isotopes in the $N = 16 - 18$ transition region [6], and several other isotopes of Al, Si and P located around the boundary of this region [4, 9, 14]. The technique involves scattering a beam of exotic nuclei with intermediate energies from a heavy target. The exotic nuclei scattered into small angles are detected in coincidence with

the prompt $\gamma$-rays de-exciting them. Small angles are selected to maximize the contribution of the Coulomb interaction in the inelastic scattering reaction. For the light nuclei studied here, the nuclear interaction contributes to the excitation cross section. From a previous study of $^{31}$Na [8] very similar to that reported here, we can estimate that the Coulomb interaction accounts for approximately 85% of the cross section in the present experiments. Detailed coupled-channels calculations for the isotopes studied here are described below.

The present measurements were performed at the National Superconducting Cyclotron Laboratory at Michigan State University. The $^{28}$Na secondary beam was produced via fragmentation of a primary beam of $^{40}$Ar at 90 MeV/nucleon from the K1200 cyclotron. The $^{30}$Na beam came from fragmentation of an 80 MeV/nucleon primary beam of $^{48}$Ca. The fragmentation of the primary beams took place in thick $^{9}$Be targets ($>$ 370 mg/cm$^2$) located at the mid-acceptance target position of the A1200 fragment separator [15]. The energies of the secondary $^{28,30}$Na beams produced in the fragmentation reactions were 43.1 MeV/nucleon and 55.6 MeV/nucleon, respectively, in the middle of the secondary target.

Thick gold foils (518 mg/cm$^2$ for $^{28}$Na and 702 mg/cm$^2$ for $^{30}$Na) were used as secondary targets. After passing through the foils, the secondary beam particles were stopped in a cylindrical fast-slow phoswich detector which provided nuclear charge identification. This charge identification, along with time-of-flight measurements in the beam line, gives positive isotope identification. For the $^{28}$Na measurement, the phoswich detector provided coverage for laboratory frame scattering angles up to 3.96°; for $^{30}$Na the maximum scattering angle was 2.80°. The corresponding scattering angles in the center of mass were 4.52° and 3.23°, respectively. The numbers of secondary beam particles collected for $^{28}$Na and $^{30}$Na were $8.2 \times 10^7$ and $3.3 \times 10^6$, respectively. The NSCL NaI(Tl) array [16] was used to detect $\gamma$-rays. The $\gamma$-ray spectra in coincidence with the detection of $^{28,30}$Na are shown in Fig. 1. While the top panels show the laboratory-frame $\gamma$-ray spectra, the spectra in the lower panels are Doppler-shifted event-by-event so they are seen as in the rest frame of the projectiles.

The projectile-frame $\gamma$-ray spectrum for $^{28}$Na shows a peak at 1240(11) keV, for which the measured cross section is 26(6) mb. Huber *et al.* [17] used laser spectroscopic techniques to determine the ground state spin of $^{28}$Na to be $J = 1$. The neighboring even-even nuclei $^{26,28}$Ne and $^{28,30}$Mg all appear to be rotational [6], so we adopt a rotational interpretation for $^{28}$Na as well. Hence, we propose that we are populating the first rotational excitation (with $J = 2$) of a $K = 1$ rotational band via an $E2$ excitation. Of course, this reaction certainly

populates the $J = 3$ member of this rotational band by an $E2$ excitation as well. However, if the 1240 keV $\gamma$-ray was the $J = 3 \rightarrow J = 1$ transition, the $J = 2 \rightarrow J = 1$ transition would have an energy less than 1240 keV and would be at least as intense. There is no evidence for such a transition in the spectrum. If the 1240 keV $\gamma$-ray was the $J = 3 \rightarrow J = 2$ transition, then the $J = 2 \rightarrow J = 1$ transition would have a smaller energy and a greater intensity. Once again, there is no evidence for such a transition. Our conclusion is that the 1240 keV $\gamma$-ray corresponds to the $J = 2 \rightarrow J = 1$ transition.

Of course, it is quite likely that the $J = 3$ member of the rotational band is also populated in the present reaction, and that the $J = 3$ state decays to the $J = 2$ state. If the rotational band is strongly coupled, then the $J = 3 \rightarrow J = 2$ transition has an energy significantly larger than 1240 keV. The $J = 3 \rightarrow J = 2$ transition is not apparent in the spectrum, but there are two factors that would conspire to suppress this transition. First, the excitation cross section for populating the $J = 3$ state is likely to be smaller than that for the $J = 2$ state. Second, the $\gamma$-ray detection efficiency decreases as the $\gamma$-ray energy increases. If the band is strongly coupled, then the energy of the $J = 3 \rightarrow J = 2$ transition is near 1800 keV. The fluctuations in the background of the measured $\gamma$-ray spectrum are consistent with such a transition.

The only prior $\gamma$-ray spectroscopic study of $^{28}$Na was performed via $\beta$-decay of $^{28}$Ne [18]. Neither of the two $\gamma$-rays observed in that study (865 and 2063 keV) were observed here. However, this is not surprising since the $\beta$-decay of the $J^{\pi} = 0^{+}$ ground state of $^{28}$Ne can only populate $J = 0$ and $J = 1$ states in the $^{28}$Na daughter nucleus.

There are two strong peaks in the projectile-frame $^{30}$Na spectrum at 433(16) keV and 701(20) keV. The apparent peak near 500 keV is quite likely to be an artifact of the 547 keV peak from the gold target. The cross sections for the two peaks are comparable (42(14) mb for the 433 keV $\gamma$-ray, 39(18) mb for the 701 keV $\gamma$-ray). However, it appears that the 701 keV $\gamma$-ray is from $^{29}$Na and is produced via single neutron stripping from the $^{30}$Na beam particle, while the 433 keV $\gamma$-ray de-excites the $J = 3$ member of the ground state $K = 2$ rotational band (the ground state spin of $J = 2$ was determined by Huber *et al.* [17]). The evidence for the assignment of the 701 keV $\gamma$-ray to $^{29}$Na comes from the energy spectrum from the phoswich detector in which the beam is stopped: the centroid of phoswich total energy signals in coincidence with the 701 keV $\gamma$-ray is lower than the centroid of $^{30}$Na energies without the $\gamma$-ray gate. Stripping cross sections of this size have been observed for

single neutron stripping reactions previously [4]. However, the $J = 4 \rightarrow J = 3$ transition between members of the ground state rotational band may also have an energy close to 700 keV. If the energy of the $J = 3$ state is 433 keV, the strong coupling model would give a $J = 4 \rightarrow J = 3$ transition energy of 577 keV. Hence, the 700 keV peak in the $\gamma$-ray spectrum may also include a contribution from the $J = 4 \rightarrow J = 3$ transition in addition to the $^{29}$Na $\gamma$-ray from single-neutron stripping.

It is important to note that the cross sections quoted here for production of $\gamma$-rays in $^{28,30}$Na are almost certainly not equal to cross sections for directly populating the first excited states. While multiple excitation (coupled channels effects) are small in these reactions [11], the second excited states in the rotational bands ($J = 3$ in $^{28}$Na and $J = 4$ in $^{30}$Na) can be excited via single-step $E2$ excitations. Therefore, the feeding of the first excited states by the second excited states must be considered in extracting electromagnetic matrix elements.

To obtain the electromagnetic matrix elements for populating excited states in $^{28,30}$Na, we used the coupled channels code ECIS88 [19], which takes into account both electromagnetic and nuclear contributions to the scattering reactions. The analyses were performed assuming the mid-target beam energies. We used standard axially symmetric deformed rotational form factors. The optical model parameters used here were obtained by Barrette *et al.* for the scattering of $^{17}$O from $^{208}$Pb at a laboratory energy of 84 MeV/nucleon [20].

There are two deformation parameters involved in each ECIS calculation. The "Coulomb deformation" $\beta_C$ reflects the deformation of the proton density in the nucleus and yields the electromagnetic matrix element $B(E2; I_{gs} \rightarrow I_f)$ via the equations [21]

$$B(E2; I_i \rightarrow I_f) = Q_0^2 e^2 \frac{5}{16\pi} < I_i K 20 | I_f K >^2 \qquad (1)$$

and

$$Q_0 = \left(\frac{16\pi}{5}\right)^{1/2} \frac{3}{4\pi} Z R_0^2 \beta_C, \qquad (2)$$

where $Q_0$ is the intrinsic quadrupole moment and $R_0 = r_0 A^{1/3}$ with $r_0 = 1.20$ fm. The "nuclear matter deformation" $\beta_A$ is used to determine the nuclear force contribution to the scattering reaction and involves transition matrix elements for both the neutrons and protons. To fit the cross section data in a unique way, we must specify the relationship between $\beta_C$ and $\beta_A$. We do this using a simple collective model picture. In such a picture,

the deformation lengths $\delta_C = \beta_C R_C$ and $\delta_A = \beta_A R_A$ are equal [22]. In these definitions of deformation lengths, $R_C = r_C A^{1/3}$ and $R_A = r_A A^{1/3}$, with $r_C$ and $r_A$ being the Coulomb radius and real nuclear radius parameters, respectively, in the optical model potentials. For the potential used here [20] the specific values are $r_A = 1.067$ fm and $r_C = 1.2$ fm. Deviations from the simple collective model picture are frequently observed in single-closed-shell nuclei [22, 23], but are highly unlikely in rotational nuclei. The direct determination of a deviation from the simple collective model picture would require a measurement using a second experimental probe, such as inelastic proton scattering (for examples of inelastic proton scattering by exotic beams, see [24–29]).

As mentioned above, it is almost certain that the second rotational excited state in each nucleus was populated in these experiments, even though $\gamma$-rays de-exciting them may not have been observed. In our ECIS analyses, we have assumed that these second rotational states ($J = 3$ in $^{28}$Na and $J = 4$ in $^{30}$Na) occur at energies which are given by the strong coupling limit. We constrain the deformation parameters for excitations of the first and second rotational states to be equal since they are assumed to be members of the same rotational bands. The experimental uncertainties we quote take into account that the second excited state in the rotational band may decay to the first excited state anywhere from 0% to 100% of the time.

The results of the ECIS analyses are given in Table I, which lists for each nucleus $\beta_C$ and $\beta_A$ deduced under the assumptions stated above, as well as the intrinsic quadrupole moments $Q_0$ and the reduced matrix elements $B(E2\uparrow)$. Figure 2(a) illustrates the evolution of the intrinsic quadrupole moments determined via intermediate energy heavy-ion scattering for the Na isotopes, including both the present study and the previously published study of $^{31}$Na [8]. To be consistent with the current analysis the value shown for $^{31}$Na in Fig. 2(a) is not extracted from the $\beta_C$ value given in Ref. [8], which assumes that 95% of the $\gamma$-ray decays from the second excited rotational state ($J = 7/2$) feed the first excited rotational state ($J = 5/2$) and that $\beta_C = \beta_A$. Instead, we have refit the experimental cross section for $^{31}$Na using the same assumptions as we did for $^{28,30}$Na. Figure 2(a) also shows intrinsic electric quadrupole moments deduced from the $\beta$-NMR measurements of spectroscopic (laboratory-frame) quadrupole moments by Keim *et al.* [30]. The intrinsic quadrupole moment $Q_0$ can be obtained from the spectroscopic quadrupole moment $Q$ via the equation [21]

$$Q_0 = Q\frac{(J+1)(2J+3)}{3K^2 - J(J+1)}. \quad (3)$$

Keim *et al.* measured the spectroscopic quadrupole moments of the ground states; therefore, $J$ and $K$ in this equation are equal. The intrinsic quadrupole moments obtained from these two methods agree for all four nuclei shown in Fig. 2(a) Despite the agreement for the individual nuclei, the trends in the two data sets seem to lead to different conclusions about the dependence of $Q_0$ on the neutron number. The heavy-ion scattering results suggest an increase in $Q_0$ as the neutron number approaches $N = 20$ ($^{31}$Na) while the $\beta$-NMR results do not suggest this increase.

One possible explanation for this apparent discrepancy is the presence of triaxiality in $^{31}$Na. As Hamamoto and Mottelson [31] point out, the ratio of the static quadrupole moment to the transition quadrupole moment is different in a triaxial nucleus than in an axially symmetric nucleus. The data shown in Fig. 2 for $^{31}$Na are not sufficient to provide strong evidence for triaxiality in this nucleus. However, measurements of transitions between higher spin members of the ground state rotational band (perhaps via direct observation of $\gamma$-rays from the fragmentation reaction in which $^{31}$Na is produced) might provide such evidence.

The first evidence for the existence of the "island of inversion" was the observation that experimental binding energies for several neutron-rich isotopes at and near $N = 20$ are larger than those calculated using the shell model with "normal" configurations, in which particles are *not* promoted across major shell gaps [1, 32–35]. Figure 2(b) shows where this deviation occurs for the Na isotopes by comparing the experimental binding energies [36–38] to the binding energies for normal configurations calculated by Warburton, Brown and Becker [1] for $^{29-33}$Na. This calculation reproduces the binding energies in $^{29,30}$Na, while $^{31,32}$Na are clearly more bound than predicted by the calculation. The trend in $Q_0$ obtained in the present study supports the conclusion suggested by the binding energies - that $^{31}$Na is in the "island of inversion" where the ground states are dominated by intruder configurations, while the lighter isotopes are not.

In summary, we have measured excitation cross section to low-lying collective states in $^{28,30}$Na and we deduced electromagnetic transition matrix elements assuming the observed transitions are de-excitations of the lowest rotational excitations of $^{28,30}$Na. The trend in the intrinsic electric quadrupole moments of Na isotopes measured using this method suggests that the ground state of $^{31}$Na is dominated by intruder configurations, while the ground

states of the lighter sodium isotopes are not. This conclusion is supported by the binding energies.

This work was supported by the National Science Foundation through grants PHY-9875122, PHY-9970991, PHY-0110253, and the State of Florida.

---

[1] E.K. Warburton, J.A. Becker and B.A. Brown, Phys. Rev. **C41**, 1147 (1990).

[2] A. Poves and J. Retamosa, Nucl. Phys. **A571**, 221 (1994).

[3] T. Motobayashi *et al.*, Phys. Lett. B **346**, 9 (1995).

[4] R.W. Ibbotson *et al.*, Phys. Rev. Lett. **80**, 2081 (1998).

[5] E. Caurier *et al.*, Phys. Rev. **C58**, 2033 (1998).

[6] B.V. Pritychenko *et al.*, Phys. Lett. B **461**, 322 (1999).

[7] Y. Utsuno *et al.*, Phys. Rev. **C64**, 011301 (2001).

[8] B.V. Pritychenko *et al.*, Phys. Rev. **C63**, 011305(R) (2001).

[9] B.V. Pritychenko *et al.*, Phys. Rev. **C62**, 051601(R) (2000).

[10] J.L. Wood *et al.*, Phys. Rep. **215**, 101 (1992).

[11] T. Glasmacher, Ann. Rev. Nucl. Part. Sci., **48**, 1 (1998).

[12] V. Chisté *et al.*, Phys. Lett. B **514**, 233 (2001).

[13] B.V. Pritychenko *et al.*, submitted to Phys. Rev. C 2002.

[14] B.V. Pritychenko *et al.*, Phys. Rev. **C63**, 047308 (2001).

[15] B.M. Sherrill *et al.*, Nucl. Inst. and Meth. **B56**, 1106 (1991).

[16] H. Scheit *et al.*, Nucl. Inst. and Meth. **A422**, 124 (1999).

[17] G. Huber *et al.*, Phys. Rev. **C18**, 2342 (1978).

[18] A.T. Reed *et al.*, Phys. Rev. **C60**, 024311 (1999).

[19] J. Raynal, Phys. Rev. **C23**, 2571 (1981).

[20] J. Barrette *et al.*, Phys. Lett. B **209**, 182 (1988).

[21] P. Ring and P. Schuck, The Nuclear Many-Body Problem, (Springer-Verlag, New York, 1980).

[22] A.M. Bernstein, V.R. Brown, and V.A. Madsen, Comments Nucl. Part. Phys. **11**, 203 (1983).

[23] A.M. Bernstein, V.R. Brown, V.A. Madsen, Phys. Lett. **103B** (1981) 255.

[24] J.H. Kelley *et al.*, Phys. Rev. **C56** (1997) R1206.

[25] J.K. Jewell *et al.*, Phys. Lett. B 454 (1999) 181.

TABLE I: Results for Coulomb ($\beta_C$) and matter ($\beta_A$) deformation parameters, intrinsic quadrupole moments ($Q_0$) and reduced electromagnetic matrix elements ($B(E2\uparrow)$). The values for the 350 keV transition in $^{31}$Na are extracted from the data [8] consistently with the analysis for $^{28,30}$Na as described in the text.

| | $\beta_C$ | $\beta_A$ | $Q_0$ (fm$^2$) | $B(E2\uparrow)$ (e$^2$fm$^4$) |
|---|---|---|---|---|
| $^{28}$Na | 0.30(7) | 0.34(8) | 33(8) | 54(26) |
| $^{30}$Na | 0.41(10) | 0.46(11) | 51(15) | $130^{+90}_{-65}$ |
| $^{31}$Na | 0.66(16) | 0.74(18) | 78(19) | $311^{+170}_{-133}$ |


[26] L.A. Riley *et al.*, Phys. Rev. Lett. 82 (1999) 4196.

[27] F. Maréchal *et al.*, Phys. Rev. C 60 (1999) 034615.

[28] H. Iwasaki *et al.*, Phys. Lett. B 481 (2000) 7.

[29] H. Scheit *et al.*, Phys. Rev. C 63 (2001) 014604.

[30] M. Keim, Proc. ENAM 98: Exotic Nuclei and Atomic Masses (Traverse City, Michigan), AIP conference proceedings **455**, 50 (1998); M. Keim *et al.*, Eur. Phys. J. A **8**, 31 (2000).

[31] I. Hamamoto and B. R. Mottelson, Phys. Lett. **B132**, 7 (1983).

[32] C. Thibault *et al.*, Phys. Rev. **C12**, 644 (1975).

[33] W. Chung and B.H. Wildenthal, Phys. Rev. **C22**, 2260 (1980).

[34] C. Détraz *et al.*, Nucl. Phys. **A394**, 378 (1983).

[35] D.J. Viera *et al.*, Phys. Rev. Lett. **57**, 3253 (1986).

[36] G. Audi *et al.*, Nucl. Phys. **A624**, 1 (1997).

[37] F. Sarazin *et al.*, Phys. Rev. Lett. **84**, 5062 (2000).

[38] D. Lunney *et al.*, Phys. Rev. **C64**, 054311 (2001).

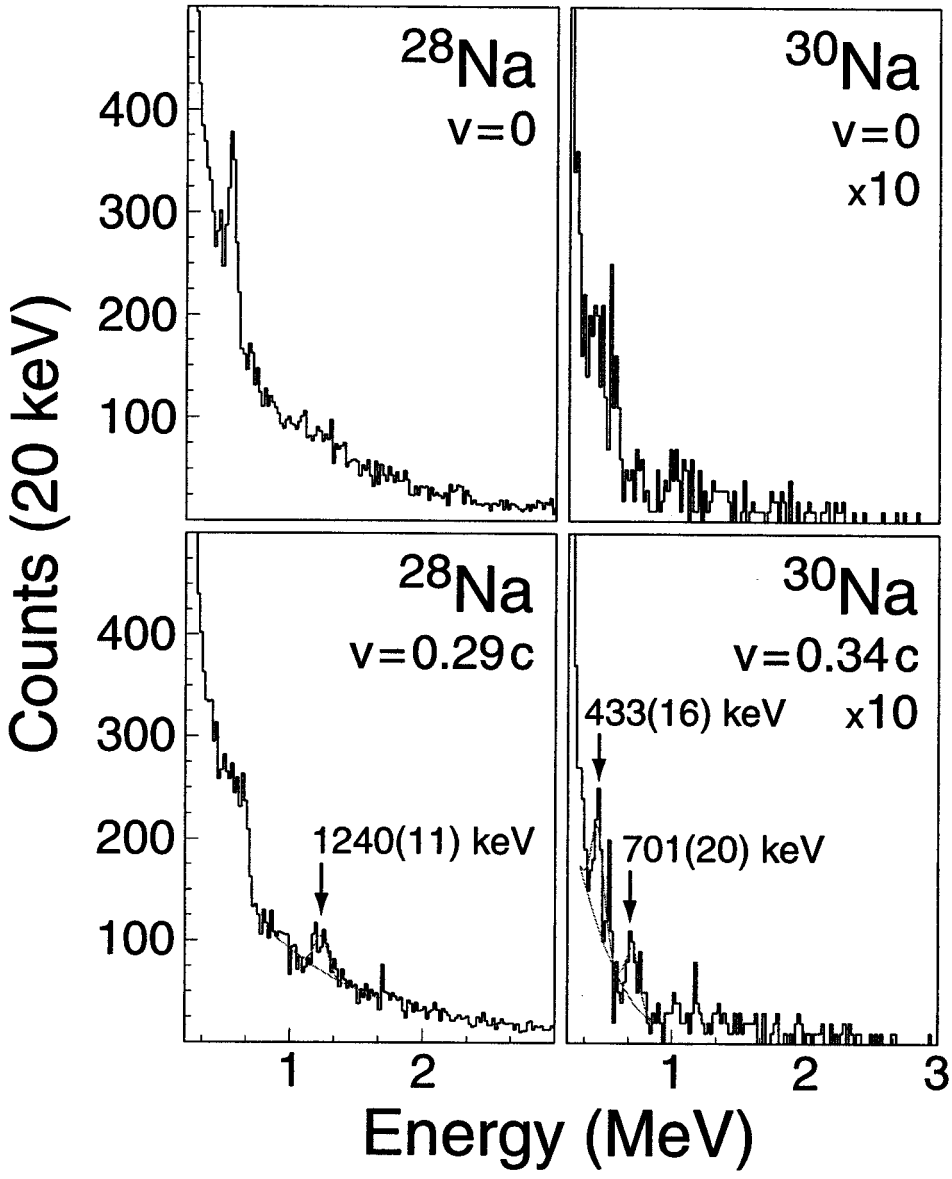


FIG. 1: Photon spectra gated on $^{28,30}$Na beams. The upper panels are laboratory-frame spectra, while the lower panels are projectile-frame spectra. The fitted peaks and backgrounds are indicated in grey.

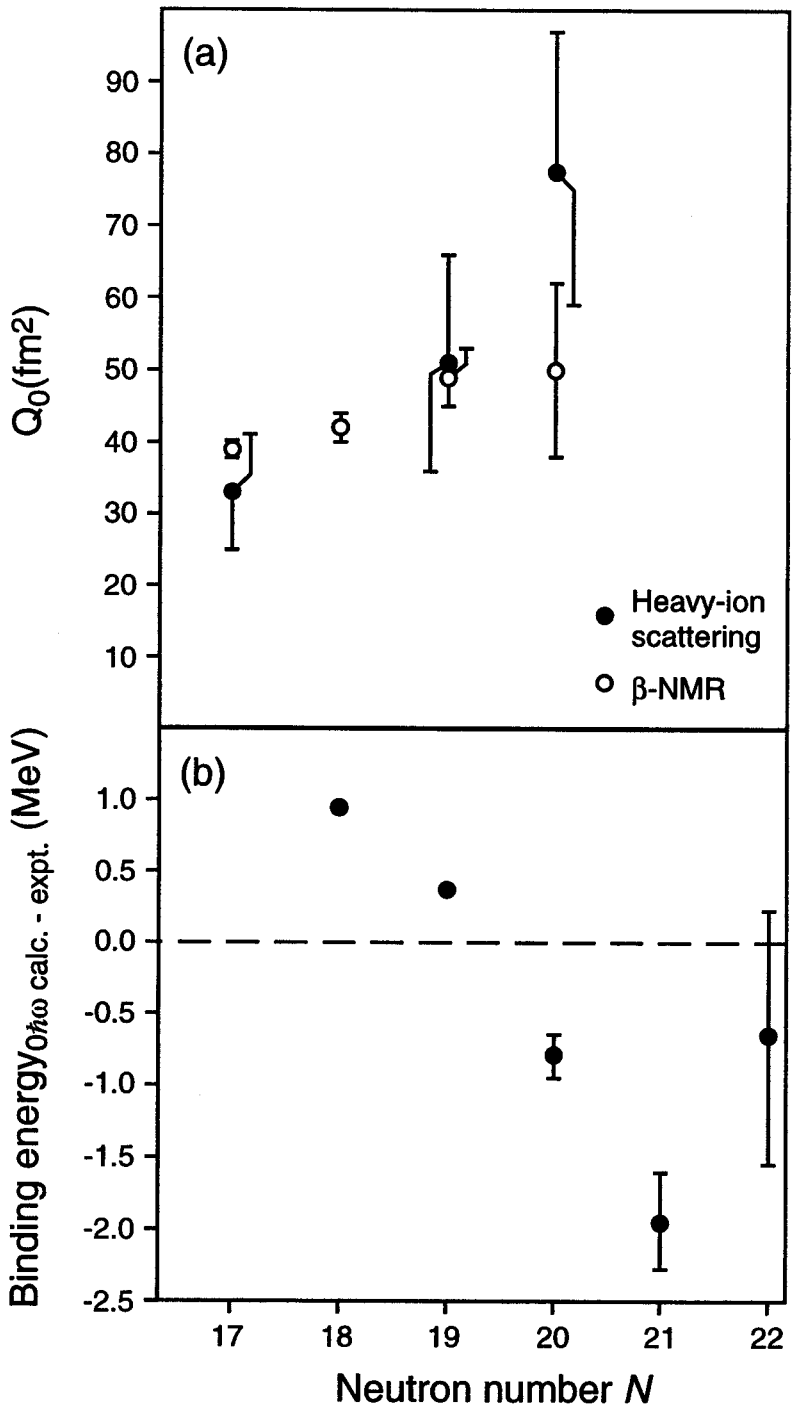


FIG. 2: (a) Intrinsic electric quadrupole moments $Q_0$ determined from the data in the present study and Ref. [8] using intermediate-energy heavy-ion scattering (solid shapes) and corresponding values determined in the study of Keim *et al.* [30]; (b) Deviation of experimental binding energies [36–38] from the calculation of Warburton, Brown and Becker [1] using "normal" ($0\hbar\omega$) configurations.